POLARIMETRY AND SHAPE FROM SHADING

Gerardo Di Martino[(1)], Alessio Di Simone[(1)], Antonio Iodice[(1)], Daniele Riccio[(1)], Giuseppe Ruello[(1)]

[(1)] Dipartimento di Ingegneria Elettrica e delle Tecnologie dell'Informazione, Università di Napoli "Federico II", Via Claudio, 21, 80125 Napoli (Italy),
Email: {gerardo.dimartino, alessio.disimone, antonio.iodice, daniele.riccio, giuseppe.ruello}@unina.it

ABSTRACT

In this paper the effects of polarimetry on the Synthetic Aperture Radar (SAR) shape-from-shading (SfS) technique developed by the authors are analysed and discussed. In particular, the validity of some hypotheses, on which the method is based, is investigated for the different polarization channels and their influence on the accuracy of the proposed SfS technique is discussed. The paper concludes providing some suggestions for polarization exploitation within the proposed technique, in order to improve overall performances.

1. INTRODUCTION

The development in the last two decades of several SAR sensors, e.g., Cosmo-SkyMed, TerraSAR-X, NovaSAR-S, Sentinel-1, etc., is a concrete proof of the increasing interest of the international scientific community in SAR imagery exploitation for the management of natural resources and monitoring of environmental hazards. Synthetic Aperture Radar certainly represents a fascinating and irreplaceable tool for these aims; indeed SAR applications very often require some kind of inversion procedure, in order to retrieve the parameter(s) of interest from the data. The inversion of SAR models is almost always a challenging problem for which no closed form solutions exist. The reason can be found in the numerous parameters influencing scattering at microwaves and then SAR data formation (see Table I). In order to provide a feasible method and then an effective inversion algorithm, a huge amount of data (i.e., several images) or some restrictive hypotheses are needed. Depending on the parameter(s) of interest, different techniques and applications have been developed.

Table I. SAR image dependencies

	Electromagnetic parameters	Geometric parameters
Surface parameters	• Dielectric constant (complex)	• Roughness • Topography (slopes)
Sensor parameters	• Polarization • Operating frequency	• Look angle • Resolution

2. SHAPE FROM SHADING

Shape from Shading, usually named also radarclinometry, is a technique developed in the computer vision field, aimed at recovering the shape of the illuminated object from a single intensity image of it. With the advent of the first SAR sensors, SfS principles were applied also to SAR images, firstly to reconstruct the underlying topography. This aim was accomplished just trying to estimate the local incidence angle or the local slopes in two orthogonal direction (typically range and azimuth) of the illuminated surface.

Despite some recent SfS techniques applied to optical data (photos) have reached very accurate results and very good performances [1], [2], very few works applied SfS principles to SAR imagery [3]-[5]. The main reason lies in the much more involved scattering phenomena at microwaves where SAR sensors typically operate. This issue represents a relevant aspect of SAR SfS and justifies why most of the literature approaches the problem simply applying optical scattering (the so-called Lambertian model [6]) to SAR images modelling. The inadequacy of the Lambertian law to properly model scattering at microwaves, together with the ill-posedeness of the problem (one equation in many unknowns), made SAR SfS doomed to fail, especially after the advent of other techniques, firstly interferometry, able to retrieve the scene topography. It is noteworthy that a proper model linking the parameters of interest (in this case the range and azimuth slopes of the surface) to the SAR data is needed. Recently [7] the authors proposed a novel SAR SfS technique based on fractal geometry. The proposed method and the effects of polarimetry on it are described in the next sections.

2.1. The proposed technique

The model proposed by the authors [7] is based on the fractal geometry both for the surface and the scattering phenomena. In particular the sensed surface, supposed natural, is modelled as a 2D fBm process, i.e., the height increments are assumed to be zero-mean Gaussian; scattering mechanisms are properly modelled via the Small Perturbation Method (SPM) applied to fractals; SAR intensity image model is then derived assuming independent scattering from different resolution cells:

$$I(\vartheta) = G\Delta x\Delta r\pi(2k)^{2(1-H)} S_0 |\beta_{mn}|^2 \frac{\cos^4 \vartheta}{(\sin\vartheta)^{3+2H}} \quad (1)$$

where G is a calibration constant, Δx and Δr are the azimuth and slant range resolutions respectively, k is the propagation constant, H is the Hurst exponent, S_0 is the spectral amplitude of the 2D fBm process, ϑ is the local incidence angle linked to the range and azimuth slopes [10]. β_{mn} is a coefficient depending on the local incidence angle and on the transmitting *(m)* and receiving *(n)* polarization:

$$\beta_{hh} = \frac{\cos\vartheta - \sqrt{\varepsilon_r - \sin^2\vartheta}}{\cos\vartheta + \sqrt{\varepsilon_r - \sin^2\vartheta}}$$

$$\beta_{vv} = (\varepsilon_r - 1)\frac{\sin^2\vartheta - \varepsilon_r(1+\sin^2\vartheta)}{\left[\varepsilon_r\cos\vartheta + \sqrt{\varepsilon_r - \sin^2\vartheta}\right]^2} \quad (2)$$

In order to simplify and speed-up the inversion procedure, the authors proposed a linearization of the direct model in (1) with respect the local slopes (small slope regime hypothesis). Since, in a first-order approximation, the SAR intensity depends only on the range slope (see [7]), in order to reintroduce the azimuth local slope, an azimuth regularization procedure is needed. In particular in [7], a Minimum Mean Squared Error (MMSE) regularization is performed.

3. EFFECTS OF POLARIMETRY

As Eqs. (1)-(2) reveal, polarimetry affects the direct model through the coefficient β_{mn} exclusively. It is clear that if all the phenomena influencing the scattering and image acquisition were taken into account properly, the estimated Digital Elevation Model (DEM) would be the same irrespective of the sent-received polarization. Polarimetry effects would be taken into account if β_{mn} variations over the scene were taken into account. This approach dramatically complicates the inversion procedure and the expansion coefficients evaluation due to the very involved dependence of β_{mn} on the local incidence angle. In order to simplify the inversion algorithm and then local slopes estimation procedure, the authors supposed the invariance of β_{mn} over the entire scene, i.e., the fundamental hypothesis $\beta_{mn}(\vartheta) = \beta_{mn}(\theta_0)$ is considered, θ_0 being the radar-look angle. As a consequence, assuming calibration constant estimated as suggested in [7] and the independence of the β_{mn} reflection coefficient from the incidence angle in the small slope regime, polarization dependency vanishes in the model.

4. EXPERIMENTAL RESULTS

Polarization effects due to the hypothesis made are analyzed and experimentally evaluated applying the proposed technique to an actual 10×10 spatial multilook SAR image of the Somma-Vesuvius complex in both HH and VV polarization (Fig. 1). The image is acquired in the stripmap mode with an operating frequency of 9.6 GHz, a radar look angle of 35° and a resolution of 2.5 m in both azimuth and ground range. The estimated DEMS are shown in Fig. 2; in Fig. 3 a comparison between reference and estimated azimuth and range profiles is performed. As can be seen, due to the polarization-independent direct model, slight differences in the estimated topography are experienced. In particular, as both Fig. 2-3 and Table II show, better results are obtained in the HH polarization. The reason lies in the behavior of the reflection coefficient, that is smoother in the HH than VV polarization with respect the local incidence angle (Fig. 4). Furthermore, the β_{mn} coefficient presents a much slower variability with respect the term $a(\vartheta) = \frac{\cos^4\vartheta}{(\sin\vartheta)^{3+2H}}$ as a function of the incidence angle, especially in the HH channel (Fig. 4). As a consequence, the angle-independence hypothesis about β_{mn} is a better approximation in the HH case.

5. CONCLUSION

An analysis of the effects of polarimetry on the SAR SfS technique proposed in [7] has been conducted. The main issue is the incidence angle-independence hypothesis about the coefficient β_{mn}, discussed in the present paper. Due to this hypothesis the proposed SfS technique experiences different performances depending on the image polarization. The flatter behavior of β_{mn} with respect the local incidence angle causes more reliable results in the HH channel. A possible approach to overcome the differences in the estimated DEMs is simply combining them, for example through a weighted averaging. A better approach would be thought if polarization issues were taken into account thus considering the variation of the β_{mn} coefficient over the image. In this way, using both HH and VV SAR image, we have two equations and two unknowns (the range and azimuth slopes) so that linearization with respect the range slope is no more required (at least in principle: ill-conditioning may arise), thus eliminating the angle-independence of β_{mn} and the small slope regime hypotheses. Another possible improvement of the proposed technique thanks to polarimetry is represented by the extension of the proposed direct model [7] to other polarization channels data through a polarimetric two-scale Small Perturbation Model (PTSM) [8], so to extend the applicability of the technique to polarimetric operative modes, also in order

to improve the accuracy of the topography estimation. A possible approach in this direction, i.e., if fully-polarimetric data are at hand, is analogous to that proposed by Chen *et al.*[9], in which shape-from-shading and polarimetric concepts are combined to estimate the range and azimuth slopes of the surface respectively.

6. REFERENCES

[1] Shimodaira, H. (2006). A shape-from-shading method of polyhedral objects using prior information. *IEEE Transactions on Pattern Analysis and Machine Intelligence*. **28**(4), 612-624.

[2] Chen, D. & Dong, F. (2010). Shape from shading using wavelets and weighted smoothness constraints. *Computer Vision, IET*. **4**(1), 1-11.

[3] Guindon, B. (1990). Development of A Shape-from-shading Technique for the Extraction of Topographic Models From Individual Spaceborne SAR Images. *IEEE Trans. Geosci. Remote Sens.* **28**(4), 654-661.

[4] Bors, A. G., Hancock, E. R. & Wilson, R. C. (2003). Terrain analysis using radar shape-from-shading. *IEEE Transactions on Pattern Analysis and Machine Intelligence.* **25**(8), 974-992.

[5] Paquerault, S., Maitre, H. & Nicolas, J.-M. (1996). Radarclinometry for ERS-1 data mapping. *Geoscience and Remote Sensing Symposium.* **1,** 503-505.

[6] Frankot, R. T. & Chellappa R. (1990). Estimation of Surface Topography from SAR Imagery Using Shape from Shading Techniques. *Artificial Intelligence.* **43** 271-310.

[7] Di Martino, G., Di Simone, A., Iodice, A., Riccio, D. & Ruello, G. (2014). On shape from Shading and SAR Images: an Overview and a New Perspective. *International Geoscience and Remote Sensing Symposium (IGARSS)*, 13-18. Quebec City.

[8] Iodice, A., Natale, A. & Riccio, D. (2011). Retrieval of Soil Surface Parameters via a Polarimetric Two-Scale Model. *IEEE Trans. Geosci. Remote Sens.* **49**(7), 2531-2547.

[9] Chen, X., Wang, C. & Zhang, H. (2009). DEM Generation Combining SAR Polarimetry and Shape-From-Shading Techniques. *IEEE Geosci. Remote Sens. Letters*, **6**(1), 28-32.

[10] Di Martino, G., Riccio, D., Zinno, I. (2012). SAR Imaging of Fractal Surfaces. *IEEE Trans. Geosci. Remote Sens.* **50**(2), 630-644.

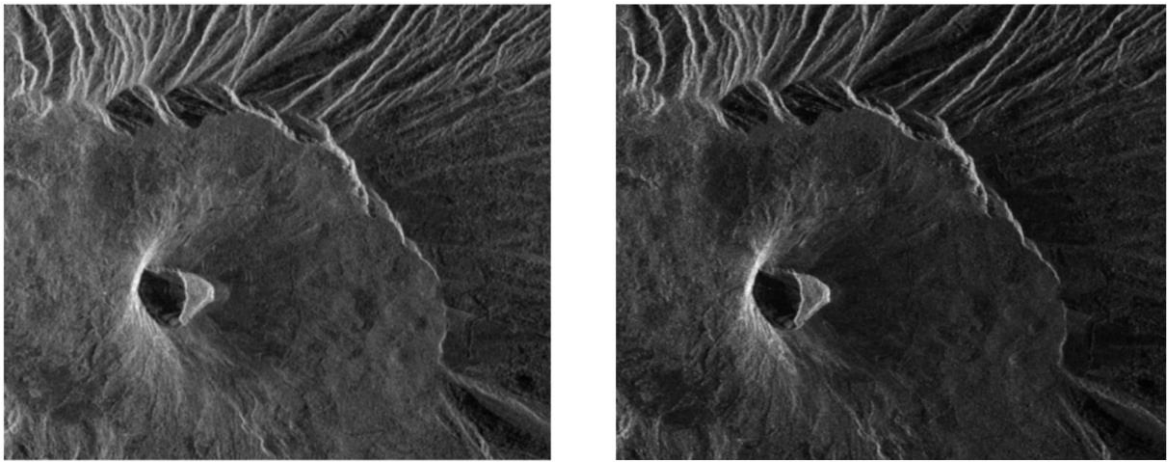

(a) (b)

Figure 1. 10×10 spatial multilook Cosmo-SkyMed SAR image acquired in the stripmap mode in HH (a) and VV (b) polarization. The operating frequency is 9.6 GHz, the radar-look angle is 35°, azimuth and ground range resolution are both equal to 2.5 m, while the pixel spacing is 2.07 m and 2.06 m in azimuth and ground range, respectively.

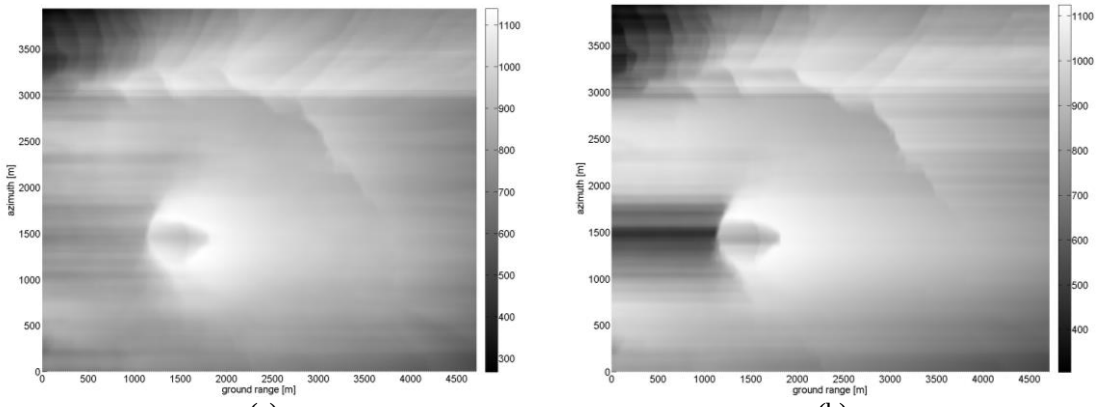

(a) (b)

Figure 2. DEM estimated in azimuth-ground range from HH (a) and VV (b) SAR images.

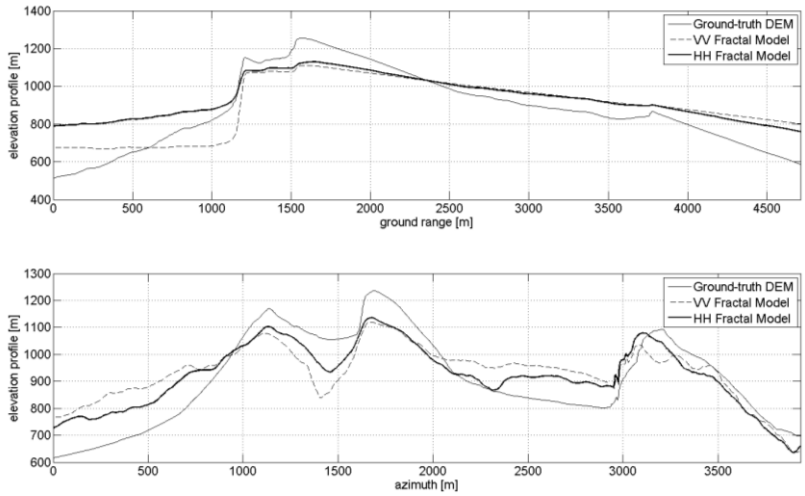

Figure 3. Comparison of range (top) and azimuth (bottom) cuts: ground-truth DEM (thin line), estimated DEM from HH (thick line) and VV (dashed line) channels.

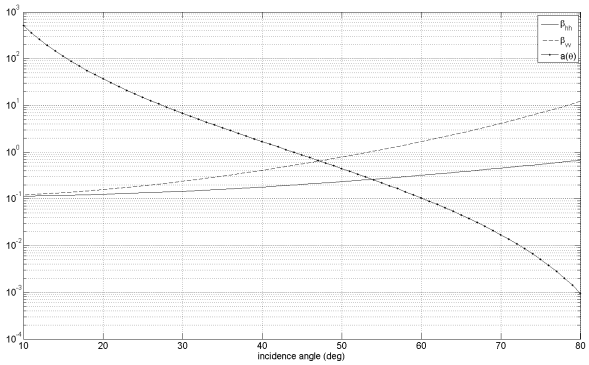

Figure 4. Module of β_{hh}, β_{vv} and $a(\vartheta)$ as a function of ϑ. The flatter behavior in HH polarization justifies the better performances in the DEM estimation.

Table II. Statistical parameters for the DEM estimated in HH and VV channels.

Error magnitude	Altitude (m)			Range slope (°)			Azimuth slope (°)		
	Median	Mean	Std dev.	Median	Mean	Std dev.	Median	Mean	Std dev.
HH	60.16	87.47	81.84	7.30	9.26	9.32	9.94	14.62	15.46
VV	68.65	104.28	106.81	9.41	11.28	10.23	11.45	17.58	18.40